International Journal of Internet, Broadcasting and Communication Vol.4 No.2 22-27 (2012)
http://dx.doi.org/10.7236/IJIBC.2012.4.2.22

IJIBC 12-2-5

Modelling the Mode Behavior of Circular Vertical-Cavity Surface-Emitting Laser

Kwang-Chun Ho[1*]

[1*]*Department of information and communication engineerin, Hansung University, Korea*
kwangho@hansung.ac.kr

Abstract

The design characteristics of circular vertical-cavity surface-emitting lasers are studied by using a newly developed equivalent network. Optical parameters, such as the stop-band or the reflectivity of periodic mirrors and the resonance wavelength, are explored for the design of these structures. To evaluate the differential quantum efficiency and the threshold current density, a transverse resonance condition of modal transmission-line theory is also utilized. This approach dramatically reduces the computational time as well as gives an explicit insight to explore the optical characteristics of circular vertical-cavity surface-emitting lasers (VCSELs).

Keywords: *Circular Modal Transmission-Line Theory, VCSELs*

1. Introduction

Since a surface-emitting laser structure was first demonstrated by Melngalis in 1965 with InSb at 10 ^{o}K [1], VCSELs have become an attractive candidate for long-haul optical communications and optical interconnect applications. This is chiefly due to their low-threshold [2], superior power transfer efficiency into single mode fibers [3], and integrability in dense two-dimensional arrays [4]. A key issue in the operation of these devices is that due to their vertical configuration the gain path-length for a single round-trip is extremely short so that the reflectivity of laser mirrors need to be high (>95 %) to achieve low-threshold current density. To understand physically the behavior of VCSELs and to give the guidance for the laser design, it is thus essential to make clear the effect of optical parameters and guiding structures on lasing characteristics.

For this purpose, Shimizu et al [5] have applied a beam propagation method (BPM) to evaluate the transverse modes of VCSELs, and Demeulenaere et al [6] have used a modal expansion of the fields satisfying Maxwell's equations to obtain a rigorous solution for the reflection properties of VCSEL's Bragg mirrors. Although these methods are accurate and can be applied to more general guiding structures, they become too laborious when carrying out 3-dimensional numerical analysis of circular VCSELs.

In this paper, we present a simple and accurate circular modal transmission-line theory (MTLT) to explore the resonance mode excited at a wavelength $\lambda_{res} = 980\,nm$. Throughout this paper, the refractive indices specifying each lossless material of the VCSEL are calculated from the literature [7] at room temperature (297 ^{o}K) and an operating wavelength $\lambda_o = 980\,nm$, where we neglect the absorption loss caused by free-carrier and inter-band absorption. Although actual indexes vary due to wavelength and material variations as well as due to the effect of gain in the pumped cavity, these calculations provide valuable insights into evaluating the properties of circular VCSELs.

Manuscript Received: Jun. 17, 2012 / Revised: Jul. 29, 2012 / Accepted: Aug. 10, 2012
Corresponding Author: kwangho@hansung.ac.kr
Tel:+82-2-760-4253, Fax: +82-2-760-4253
Dept. of information and communication engineering, Hansung University, Korea

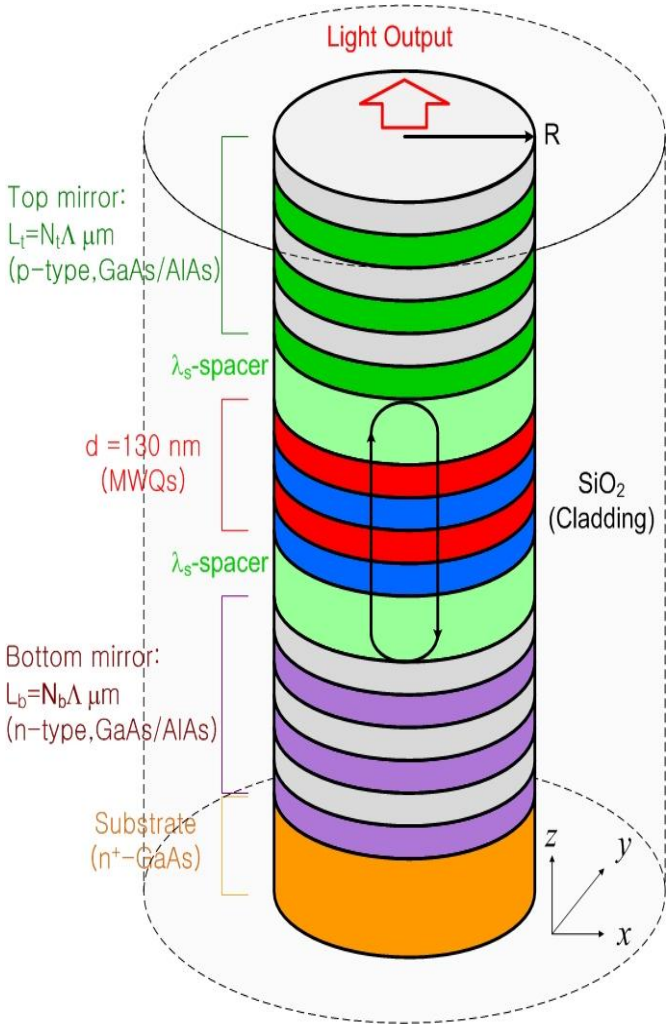

Fig. 1. A typical 3-D circular vertical-cavity laser with 3 quantum wells and core layers of width W, where $p \approx 2\times10^{19}\,cm^{-3}$, $n \approx 10^{18}\,cm^{-3}$, $n^+ \approx 6\times10^{18}\,cm^{-3}$. Then, the calculated refractive indices of p- and n-type (GaAs, AlAs) are (3.494, 3.323) and (3.498, 3.322), respectively.

2. Modal Characteristics of Circular VCSELs

The optical properties of circular VCSELs are strongly dependent on the selectivity of transverse modes. In general, the mode selectivity is achieved by cladding a material like SiO_2 with a low refractive index around the core layers (with width W) of VCSELs. Such a generic 3-D circular VCSEL structure used widely to improve the thermal and the electrical resistance is illustrated in Fig. 1. It is comprised of two components: a top and a bottom distributed Bragg reflector (DBR) mirror, and a center active/spacer region. The planar top and bottom mirrors include symmetric $N_t = 40$ and $N_t = 45$ pairs of alternating quarter-wavelength $\lambda_o/4n$(where n is the refractive index of the alternating material) stacks of GaAs/AlAs DBR, respectively. Also, the active region consists of $In_{0.2}Ga_{0.8}As$/GaAs with 3-quantum wells placed at the center of $Al_{0.4}Ga_{0.6}As$ λ_s-spacers (where $\lambda_s = \lambda_o/n_s$with the refractive index $n_s$and the thickness of wells is $t_m = 10\,nm$).

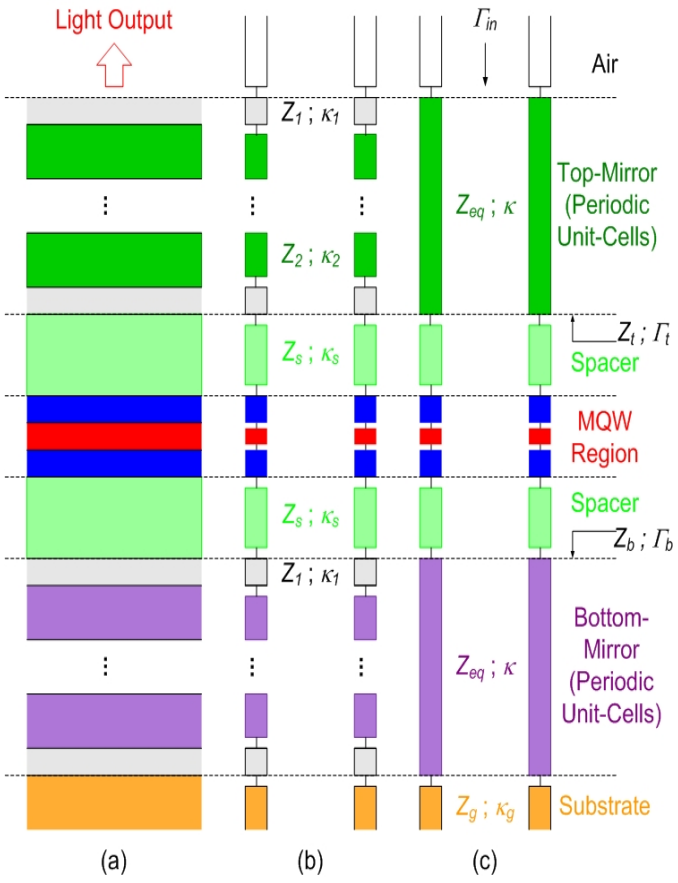

Fig. 2. Schematic configurations of (a) the 2-D circular VCSEL structure, (b) the conventional network approach, and (c) the reduced network approach satisfying Floquet's theorem.

To find the input reflectivity Γ_{in} of a typical circular VCSEL looking down at the top-window, there are two possible transmission-line network representations. They are either a conventional network comprised of the corresponding transmission-line segments for every layer or a reduced network satisfying circular MTLT, as depicted in Fig. 2(b) and (c), respectively. The former network takes a long computational time due to the large number of segments required to describe the multilayered structure, while the latter is simple and convenient in formulation. In this subsection, we thus define the equivalent characteristic impedance Z_{eq} for a reduced network, which will be adopted to evaluate the power reflection in top and bottom DBR mirrors. For the purpose of convenient network construction, we apply the bisection principle to the network of Fig 2(b) at the symmetric plane. Then, the input impedance for open-bisection is given by

$$Z_{ob} = iZ_1 \frac{Z_2 - Z_1 \tan(\kappa_1 \Lambda_1 / 2)\tan(\kappa_2 \Lambda_2 / 2)}{Z_1 \tan(\kappa_2 \Lambda_2 / 2) + Z_2 \tan(\kappa_1 \Lambda_1 / 2)} \quad , \tag{1}$$

where the subscript *ob* represents the abbreviation of open-bisection. On the other hand, the electric field of odd type is equal to zero at the symmetric bisected plane so that a electric conducting wall is placed at that plane, and the equivalent network is terminated by short-circuit. Then, the input impedance becomes

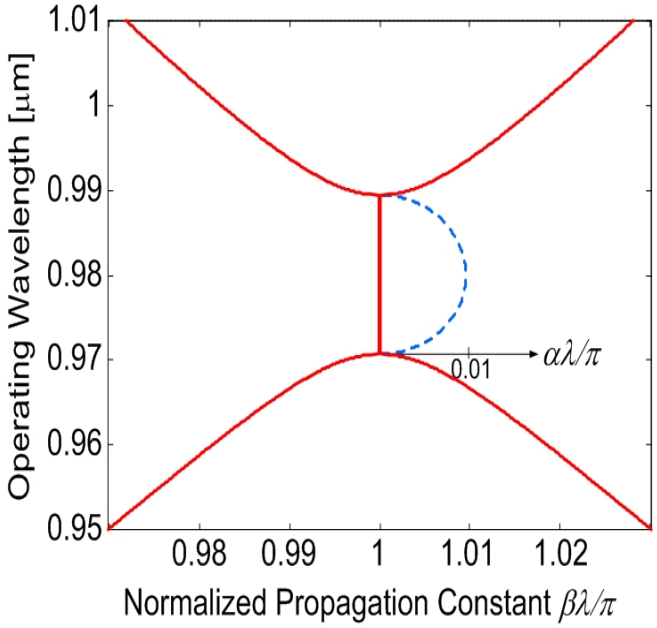

Fig. 3. Dispersion curves for top and bottom mirrors, where the dashed-lines represent the normalized attenuation factors.

$$Z_{sb} = -iZ_1 \frac{Z_1 \tan(\kappa_1 \Lambda_1 / 2) + Z_2 \tan(\kappa_2 \Lambda_2 / 2)}{Z_1 - Z_2 \tan(\kappa_1 \Lambda_1 / 2)\tan(\kappa_2 \Lambda_2 / 2)} \quad , \tag{2}$$

where the *sb* stands for short-bisection. Consequently, the equivalent characteristic impedance Z_{eq} for a symmetric unit-cell of periodic structures can be expressed as

$$Z_{eq} = \sqrt{Z_{ob} Z_{sb}} \quad . \tag{3}$$

Similarly, the normalized equivalent propagation constant of Fig. 2(c) ($\kappa\Lambda/\pi$) can be obtained by

$$\frac{\kappa\Lambda}{\pi} = \frac{1}{\pi}\cos^{-1}\left[\theta(\lambda)\right] \quad , \tag{4}$$

where the dispersion parameter $\theta(\lambda)$ is defined as

$$\theta(\lambda) = \cos(\kappa_1\Lambda_1)\cos(\kappa_2\Lambda_2) - \frac{1}{2}\left(\frac{n_1^2 + n_2^2}{n_1 n_2}\right)\sin(\kappa_1\Lambda_1)\sin(\kappa_2\Lambda_2) \quad . \tag{5}$$

The dispersion relation derived in Eq. (5) is numerically evaluated for the top and bottom DBR mirrors consisted of lossless p- and n-type GaAs/AlAs layers. To achieve the resonance along the longitudinal z-direction of a single transverse mode, the width of guiding cores is selected as $W = 0.16\ \mu m$. Under this condition, the eigenvalue problem of transverse resonance condition produces accurate propagation constants κ_1, κ_2 for each local section. Figure 3 shows that the 1st-order Bragg stop-band occurs at a normalized attenuation factor $\alpha\lambda/\pi \approx 0.01$ for both mirrors at an operating wavelength $\lambda_o = 980\ nm$, where the solid-line represent the real components of normalized propagation constant $\kappa\Lambda/\pi$, while the dashed-lines

show the imaginary components (attenuation factors).

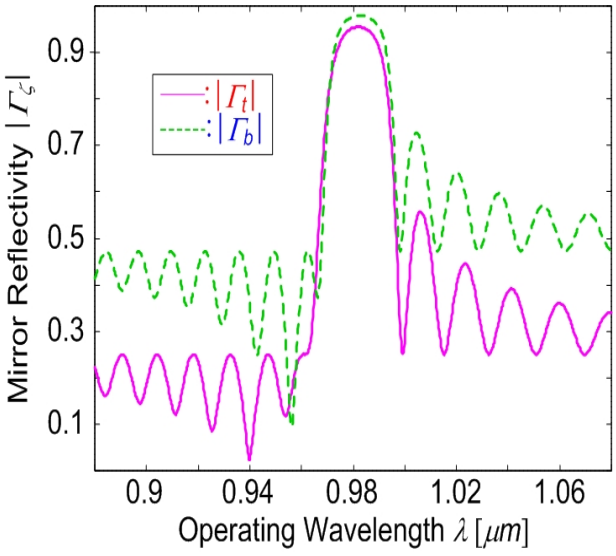

Fig. 4. Power reflection as a function of wavelength, where the solid-line and the dashed-line are for top and bottom mirrors, respectively.

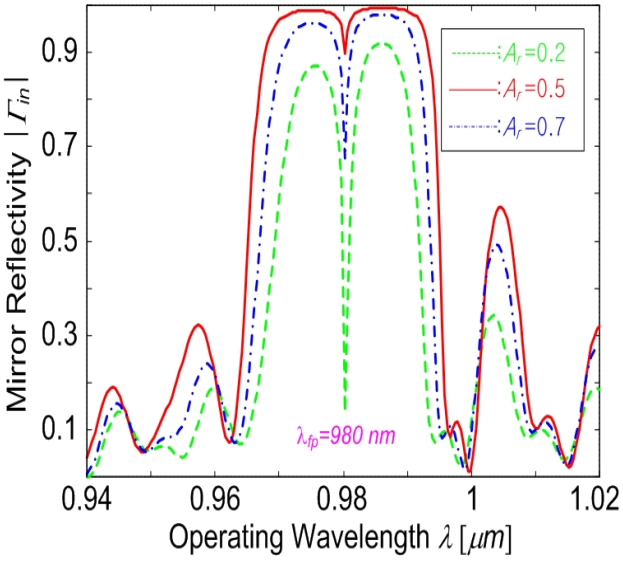

Fig. 5. Calculated spectral reflectivity for TE modes of the circular VCSEL pictured in Fig. 1, where is the aspect ratio and is the resonance mode.

3. Design Characteristics and Numerical Results

In section 2, we defined the equivalent propagation constant κ, and the characteristic impedance $Z_{es}$for top (and bottom) periodic DBR mirrors consisted of symmetric unit-cells of 40 (and 45) pairs, respectively, with quarter-wavelength thickness ($\Lambda_1 =$, $\lambda_o/4n_1\ \mu m$, $\Lambda_2 = \lambda_o/4n_2\ \mu m$). Using these modal characteristics, we evaluate simply and accurately the reflectivity for TE modes of those mirrors looking up (and down) at λ_s-spacers. As shown in the analytic equivalent networks of Fig. 2(c), the reflection coefficient is then given by

$$\Gamma_{\varsigma} = \frac{Z_{\varsigma} - Z_s}{Z_{\varsigma} + Z_s} \quad , \tag{6}$$

where Z_{ς}represents the input impedance looking up and down at the spacers, respectively, with ς=*t* or *b*. Figure 4 shows that the reflectivity is 0.955 and 0.979 for the top and bottom mirrors, respectively, at a wavelength $\lambda_o = 980\,nm$. Therefore, this vertical-cavity laser emits the output light through top-window because the reflectivity of top mirrors is smaller than that of the bottom mirrors.

Next, we evaluate numerically the input reflectivity for TE modes looking down from the top-window of circular VCSEL when each individual layer is not exactly quarter-wave. Figure 5 shows that there is a single Fabry-Perot mode with resonance wavelength $\lambda_o = 980\,nm$in DBR mirror bandwidth, and a significant degradation of peak reflectivity and spectral bandwidth can occur when the aspect ratio Ar is detuned to 0.2 and 0.7 at in-phase value 0.5. Here, the aspect ratio Ar=0.7 means that when the GaAs layer is 40% more than a designed value of $\Lambda_2 = \lambda_o/4n_2\,\mu m$, the AlAs is 40% thinner than $\Lambda_1 = \lambda_o/4n_1\,\mu m$. The aspect ratio is then defined by

$$A_r = \frac{1}{n_1 - n_2}\left[\frac{2\Lambda}{\lambda_o} - n_1\right] \quad . \tag{7}$$

It is easy to see here that the periodicity of alternating material is given as $\Lambda = \lambda_o/4n_1 + \lambda_o/4n_2\,\mu m$at in-phase condition of propagation mode.

4. Conclusion

We have analyzed a typical circular VCSEL operating at a resonance wavelength with circular modal transmission-line theory (MTLT). The dispersion relation has shown that the planar top and bottom DBR mirrors have a stop-band at first-order Bragg condition (), and produce a Fabry-Perot (FP) mode in the spectral bandwidth. These overall results reveal that the circular MTLT can be served as a convenient and powerful approach for the studies of circular VCSELs having lossy or gainy materials.

References

[1] L. Melngalis, “Longitudinal Injection-Plasma Laser of InSb,” Appl. Phys. Lett., Vol.6, No.3, pp.59-60, 1965.
[2] R. S. Geels, S. W. Corzine, J. W. Scott, D. B. Young, and L. A. Coldren, “Low Threshold Planarized Vertical-Cavity Surface-Emitting Lasers,” IEEE Photon. Technol. Lett., Vol.2, No.4, pp.234-236, 1990.
[3] K. Tai, G. Hasnain, J. D. Wynn, R. J. Fischer, Y. H. Wang, B. Weir, J. Gamelin, and A. Y. Cho, “90 % Coupling of Top Surface Emitting GaAs/AlGaAs Quantum Well Laser Output into 8 *mm* Diameter Core Silica Fire,” Electron. Lett., Vol.26, No.19, pp.1628-1629, 1990.
[4] C. J. Chang-Hasnain, J. P. Harbison, Chung-En Zah, M. W. Maeda, L. T. Florez, N. G. Stoffel, and Tien-Pei Lee, “Multiple Wavelength Tunable Surface-Emitting Laser Arrays,” IEEE J. Quantum Electron., Vol.27, No.6, pp.1368-1376, 1991.
[5] M. Shimizu, F. Koyama, and K. Iga, “Transverse mode analysis for surface emitting laser using beam propagation method,” IEICE Trans., E-74, No.10, pp.3334-3341, 1991.
[6] B. Demeulenaere, D. De Zutter, and R. Baets, “Rigorous Electromagnetic Study of Diffraction Loss in VCSEL Mirrors,” IEE Proc. Optoelectron., Vol.143, No.4, pp.221-227, 1996.
[7] K. C. Ho, G. Griffel and T. Tamir, “Polarization Splitting in Lossy/Gainy MQW Directional Couplers,” J. Lightwave Technol., Vol.LT-15, pp.1233~1240, 1997.